Conversion of evanescent into propagating light in near-field scanning optical microscopy

doi: 10.1063/1.362551

Conversion of evanescent into propagating light in near-field scanning optical microscopy

Kenji Fukuzawa[a] and Hiroki Kuwano
NTT Interdisciplinary Research Laboratories, 3-9-11 Midori-cho, Musashino-shi, Tokyo 180, Japan

(Received 3 November 1995; accepted for publication 29 February 1996)

Conversion of evanescent light into propagating light (as needed in near-field scanning optical microscopy) is analyzed by means of a photocantilever. The photocantilever is a silicon cantilever with a *pn* junction photodiode on its tip. The photocantilever tip converts evanescent light from a sample into propagating light. Theoretical values given by scattering and transmission models are compared with our experimental values. The scattering model gives results that are closer to the experimental values than does the transmission model. This indicates that the nonpropagating evanescent light is converted into scattered light at the photocantilever tip, and that the scattered light is collected by the photodiode. © *1996 American Institute of Physics.* [S0021-8979(96)07411-7]

I. INTRODUCTION

The resolution of conventional optical microscopy is limited to about half the wavelength of the light source because of light diffraction. Near-field scanning optical microscopy (NSOM), a type of scanning probe microscopy, is expected to provide optical characteristic distributions of samples with nanometer lateral resolution.[1–5] Photon scanning tunneling microscopy[6–8] (PSTM) or scanning tunneling optical microscopy[9] (STOM) uses evanescent light illumination. In these types of microscopy, a sharpened fiber probe or a microfabricated probe (currently used for atomic force microscopy) converts nonpropagating evanescent light from a sample into propagating light. This light is then collected with a detector that is placed a certain distance from the probe. The conversion from evanescent light into propagating light is the key process in evanescent-illumination NSOMs.

We recently proposed a new semiconductor-based NSOM/atomic force microscopy (AFM) probe,[10] which we call a photocantilever. It consists of a microfabricated silicon cantilever with a *pn* junction photodiode at its tip. Since the photodiode is placed close to the probe tip, the photocantilever has a larger acceptance angle for collecting the light from the probe tip than the setup reported by van Hulst *et al.*[8] It is also suitable for mass production. The sample is illuminated with non-propagating evanescent light provided by total internal reflection (TIR) from a prism surface, as is done in PSTM. The cantilever tip then converts the evanescent light transmitted from the sample into propagating light. The photodiode at the tip of the photocantilever collects the propagating light. With this photocantilever-based NSOM, 20 nm gaps between small particles have been resolved,[11] even though the photodiode area was over 100 μm^2. In addition, the cantilever did not have any fabricated microprotrusions. Conversion from nonpropagating evanescent light into propagating light is the most significant process for a photocantilever based NSOM. In this article we experimentally and theoretically investigate this conversion process.

[a]Electronic mail: fukuzawa@ilab.ntt.jp

II. RESULTS AND DISCUSSION

A. Experimental setup

Figure 1(a) illustrates the photocantilever-based near-field optical signal measurement system. The details of the photocantilever are explained in Refs. 10 and 11. The incident beam is totally reflected by the prism surface, and the sample on the prism is illuminated by the evanescent wave. The tip of the photocantilever perturbs the evanescent light from the sample and converts it into a propagating wave. This light is converted into a photocurrent by a photodiode on the cantilever tip. The photocantilever is 1500 μm long, 100 μm wide, and 5 μm thick. The 5 μm thickness was needed for sufficient light absorption, because the light penetration depth of silicon is 4 μm for light with a wavelength of 670 nm. The large size relative to commercially available cantilevers was required to obtain a spring constant of less than 1 N/m with a thickness of 5 μm. Figure 1(b) shows the structure of the photocantilever tip. The triangular region in the figure is the *pn* junction photodiode area. Both the height and the base length of this area are about 10 μm. The depth of the *pn* junction is about 1 μm. The surface that faces the sample is coated with a 220-nm-thick SiO_2 antireflection layer. In this experiment, we used a cantilever without any fabricated microprotrusions. A 5 mW He–Ne laser was used as a light source (λ:633 nm), and the incident angle was set at 45°. The electric field vector of the light was rotated by using a $\lambda/2$ plate. In this experiment, the sample was not placed on the prism; so, the cantilever tip contacted the prism surface.

B. Theoretical evaluation

We analyzed two possible ways of converting the evanescent light into propagating light: transmission and scattering. These two models are shown in Fig. 2. The probe size was assumed to be infinitely large in the transmission model; the cantilever tip was assumed to be an infinite plane. The evanescent light is transmitted from the prism into the photocantilever as light transmitted between two parallel infinite plates separated by air. In contrast, the probe size is assumed

 0021-8979/96/79(11)/8174/5/$10.00

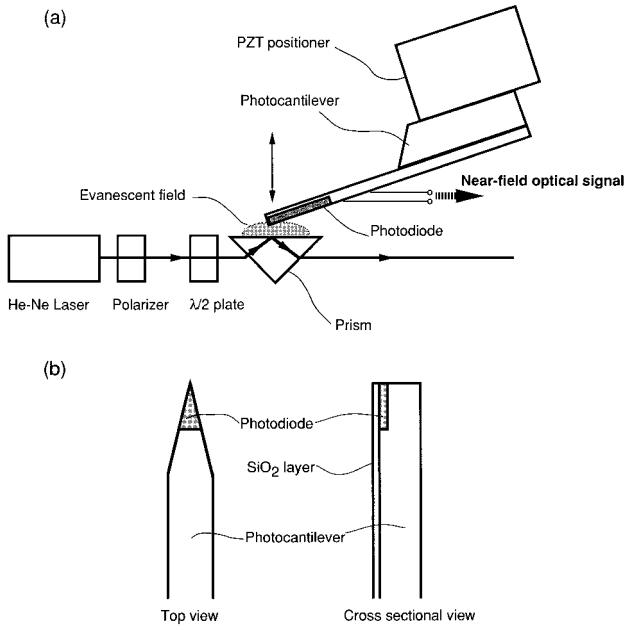

FIG. 1. (a) Setup of the photocantilever-based near-field optical measurement system. (b) Schematic structure of the photocantilever.

to be infinitely small in the scattering model; the cantilever tip was assumed to be a point. The evanescent light is scattered at the cantilever tip, and the scattered light is collected by the photodiode on the cantilever. We compared experimental and theoretical results for two basic NSOM characteristics: the dependency of the incident light polarization and the decay characteristics as a function of the gap between the prism and the photocantilever.

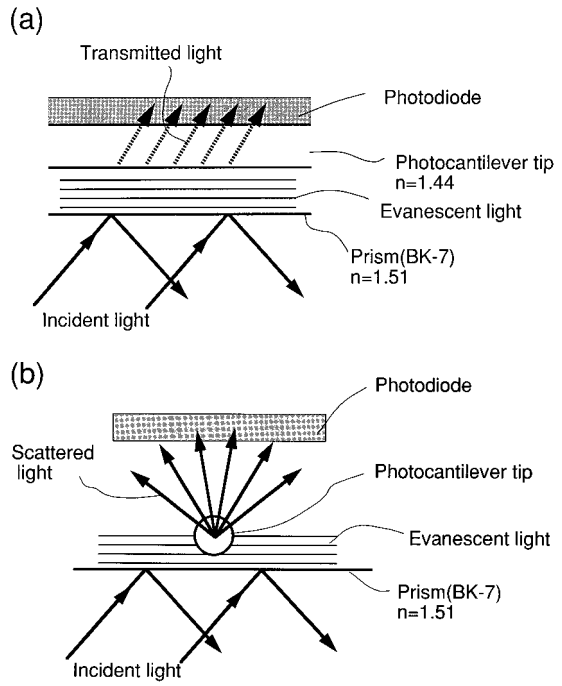

FIG. 2. Models of the process for conversion from evanescent light into propagating light. (a) Transmission model. The probe size is assumed to be infinitely large. The evanescent light is transmitted from the prism into the photocantilever as light transmitted between two parallel infinite plates separated by air. (b) Scattering model. The probe size is assumed to be infinitely small. The evanescent light is scattered at the cantilever tip.

1. Transmission model

In the transmission model the intensity of the transmitted light was assumed to be proportional to the transmittance of the two parallel infinite plates separated by air. This assumption was also made for the theoretical evaluation of PSTM.[12] The size of the photocantilever was assumed to be infinite. The method using the characteristic matrix for a stratified media was used to obtain the transmittance.[13] This method accounts for multiple reflections. The transmittance for the gap z between the cantilever and the prism for p- and s-polarized light, $T_p(z)$ and $T_s(z)$, is

$$T_p(z) = \frac{n_3 \cos\theta_1}{n_1\sqrt{1-n_{13}^2\sin^2\theta_1}}\left|\frac{2p_0}{p_0 m_{11}+p_0 p_s m_{12}+m_{21}+p_s m_{22}}\right|^2, \tag{1}$$

$$T_s(z) = \frac{n_3\sqrt{1-n_{13}^2\sin^2\theta_1}}{n_1\cos\theta_1}\left|\frac{2q_0}{q_0 m_{11}+q_0 q_s m_{12}+m_{21}+q_s m_{22}}\right|^2, \tag{2}$$

where n_1 and n_3 are the refractive indices of the prism and the cantilever, $n_{ij}=n_i/n_j$, θ_1 is the incident angle of the laser beam, $p_0 = n_1/\cos\theta_1$, $p_s = n_3/\sqrt{1-n_{13}^2\sin^2\theta_1}$, $q_0 = n_1\cos\theta_1$, and $q_s = n_3\sqrt{1-n_{13}^2\sin^2\theta_1}$. Here, m_{ij} is the element of the following characteristic matrixes M_p and M_s for p and s polarizations:

$$M_p = \begin{pmatrix} \cos\gamma z & \dfrac{-i\sin\gamma z}{p} \\ -ip\sin\gamma z & \cos\gamma z \end{pmatrix}, \tag{3}$$

$$M_s = \begin{pmatrix} \cos\gamma z & \dfrac{-i\sin\gamma z}{q} \\ -iq\sin\gamma z & \cos\gamma z \end{pmatrix}, \tag{4}$$

where $\gamma = ikn_2\sqrt{n_{12}^2\sin^2\theta_1-1}$, $p = n_2/(i\sqrt{n_{12}^2\sin^2\theta_2-1})$, $q = in_2\sqrt{n_{12}^2\sin^2\theta_2-1}$, and n_2 is the refractive index of air. In this evaluation, $n_1=1.51$ and $n_3=1.44$, since the prism is made of BK-7 glass and the 220-nm-thick antireflection SiO_2 layer of the photocantilever faces the prism.

2. Scattering model

For light scattering analysis, the scattered light was assumed to be the field radiated by a point dipole in the evanescent field. Part of the radiated light is collected by the detector. Since the cantilever tip is assumed to be infinitely small in this model, it does not perturb the evanescent field generated at the air–prism interface. Therefore, the intensity of the evanescent field decays exponentially according to $\exp(-2i\gamma z)$, where z is the distance from the prism surface.

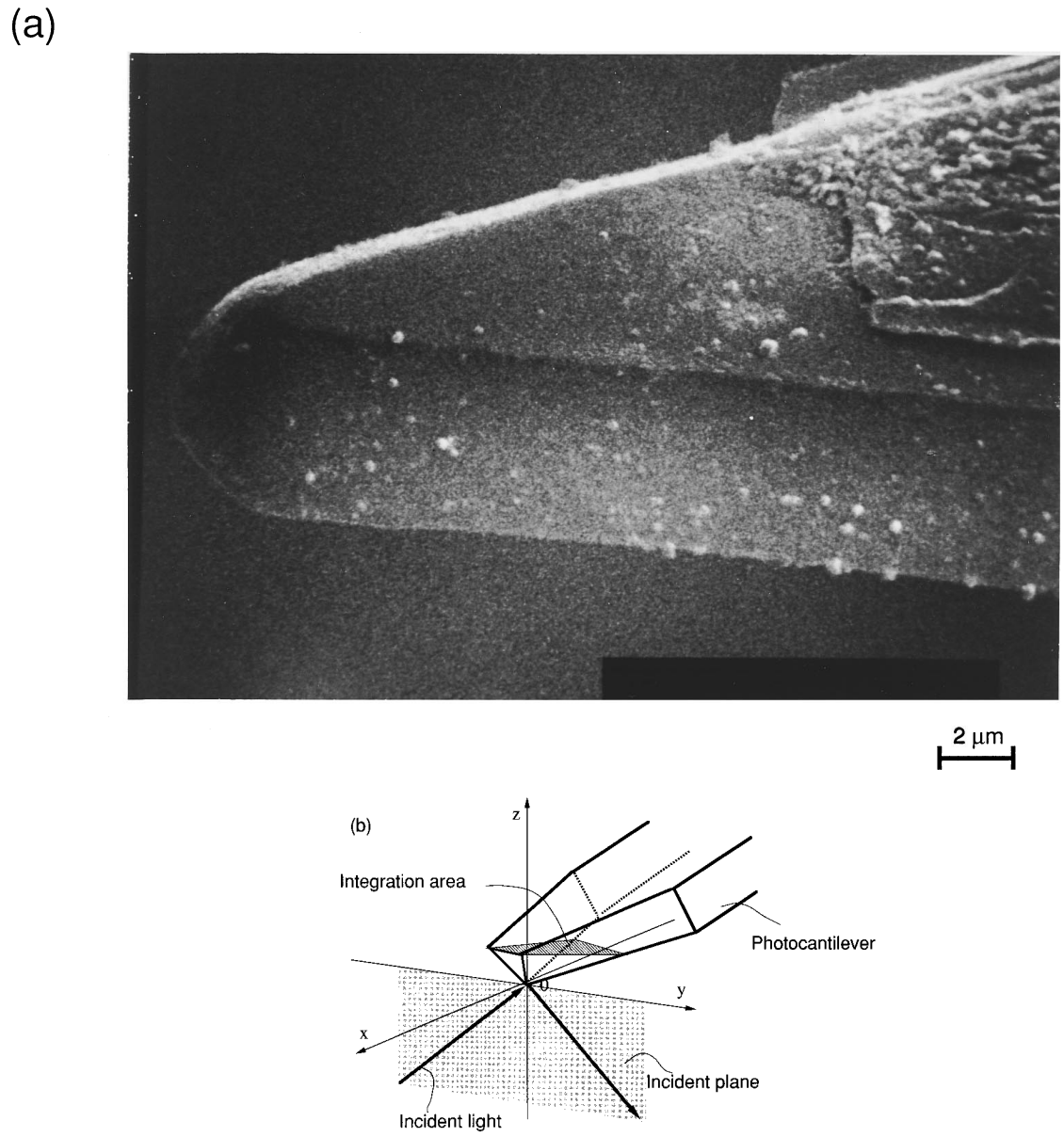

FIG. 3. Shape of the photocantilever tip. (a) Scanning electron micrograph of the photocantilever tip. The photodiode was fabricated on the upper plane in the photograph. (b) Model for calculation based on light scattering. The prism surface is on the xy plane; the incident plane is on the yz plane. The long axis of the cantilever is parallel to the x axis, and the cantilever tip is on the origin. The photodiode side faces the xy plane.

In addition, isotropic susceptibility was assumed; therefore, the magnitude of the dipole moment was assumed to be proportional to the evanescent electric field amplitude. The amplitude of the evanescent field at $z=0$ (when the cantilever contacts the prism) was assumed to be proportional to the value obtained by Fresnel's amplitude transmittance equations when the light is transmitted from the prism into air. In general, the electromagnetic fields radiated by a point dipole can be expressed as

$$\mathbf{E}=\frac{1}{4\pi\epsilon_0}\left[k^2(\mathbf{n}\times\mathbf{p})\times\mathbf{n}\frac{e^{ikr}}{r}+[3\mathbf{n}(\mathbf{n}\cdot\mathbf{p})-\mathbf{p}]\left(\frac{1}{r^3}-\frac{ik}{r^2}\right)e^{ikr}\right], \tag{5}$$

$$\mathbf{H}=\left(\frac{\epsilon_0}{\mu_0}\right)^{1/2}\frac{k^2}{4\pi\epsilon_0}(\mathbf{n}\times\mathbf{p})\frac{e^{ikr}}{r}\left(1-\frac{1}{ikr}\right), \tag{6}$$

where $\mathbf{p}$ is the vector of the dipole moment and k is the wave number.[14] Here r and $\mathbf{n}$ are the distance and the unit vector of the observation point from the origin. When $kr\gg1$, Eqs. (5) and (6) can be rewritten as

$$\mathbf{E}=\frac{k^2}{4\pi\epsilon_0}(\mathbf{n}\times\mathbf{p})\times\mathbf{n}\,\frac{e^{ikr}}{r}\quad(kr\gg1), \tag{7}$$

$$\mathbf{H}=\left(\frac{\epsilon_0}{\mu_0}\right)^{1/2}\frac{k^2}{4\pi\epsilon_0}(\mathbf{n}\times\mathbf{p})\frac{e^{ikr}}{r}\quad(kr\gg1). \tag{8}$$

Equations (7) and (8) indicate that the radiated field intensity has different angular distributions for s and p polarizations.

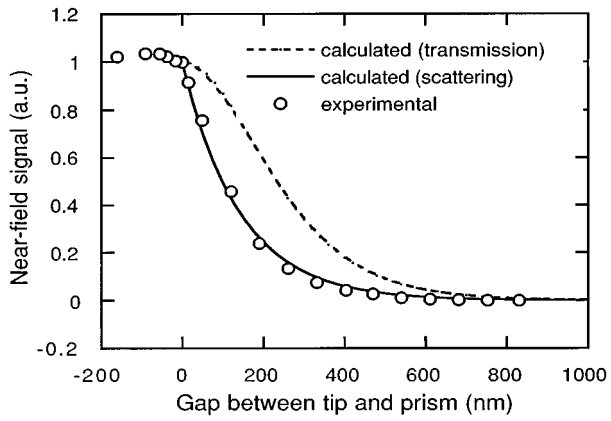

FIG. 4. Relationship between the near-field optical signal and the gap between the photocantilever and prism.

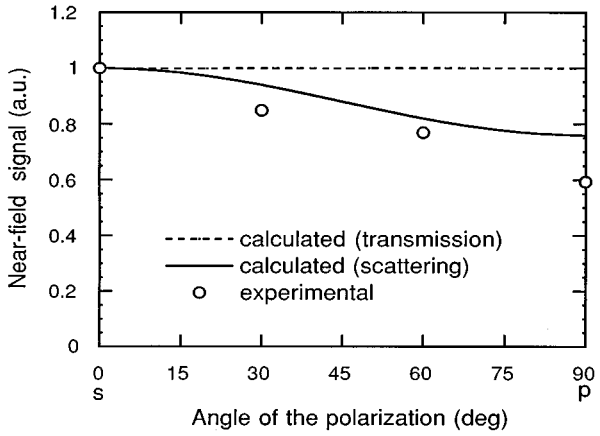

FIG. 5. Polarization dependence of the near-field optical signal.

The photodiode collects part of the radiated field. The amount of the light that can be collected with the photodiode is determined by the geometry of the photodiode region of the cantilever. Therefore, the Poynting vector was integrated over the solid angle obtained for the actual geometrical arrangement to obtain the total power detected with the photodiode P,

$$\mathbf{P}=\tfrac{1}{2}\int_{\Delta\Omega} d\Omega\ \mathrm{Re}[r^2\mathbf{n}\cdot(\mathbf{E}\times\mathbf{H}^*)]. \tag{9}$$

Here $\mathbf{H}^*$ denotes the complex conjugate of $\mathbf{H}$. Figure 3 shows the integration region of the Poynting vector. Figure 3(a) is a scanning electron microscope (SEM) photograph of the photocantilever tip. The photodiode was fabricated on the upper plane in the photograph. The fabricated side wall is not vertical, but is at an angle to the photodiode surface.[10] In addition, a submicron size asperity at the cantilever tip can be seen. Based on the actual shape of the cantilever [Fig. 3(a)], we estimated the integration area of the Poynting vector flowing into the plane [the trapezoid in Fig. 3(b)]. The prism surface is on the xy plane ($z=0$), and the incident plane is on the yz plane ($x=0$). The long axis of the cantilever is parallel to the x axis, and the cantilever tip is on the origin. The cantilever is slanted 15° to the prism surface. The directions of the dipole moment are parallel to the x and z axes for the s and p polarizations, respectively. The photodiode side faces the xy plane. Note that the upper plane of the cantilever faces the sample in Fig. 3(a).

C. Experimental results

Figure 4 shows the relationship between the near-field optical signal and the gap between the photocantilever and prism. The solid and dotted lines represent the values given by the scattering and transmission models, for p polarization. The circles represent the experimental values for p polarization. The horizontal axis shows the z-scan control signal. The values given by the scattering model agree well with the experimental values, but the values given by the transmission model do not.

Figure 5 shows the near-field optical signal as a function of the polarization angle. The solid and dotted lines represent the values given by the scattering and the transmission models, respectively. The circles represent experimental values. In the figure, 0° and 90°, respectively, correspond to the s and p polarization incidence. The plotted optical signals are for the case when the cantilever contacts the prism surface. In the transmission model, the dependency on the polarization is weak since the evanescent light is transmitted between the materials with similar refractive indexes (from the prism to the SiO_2 layer, as mentioned Sec. II B 1). These data indicate that the scattering model gives values that are closer to the experimental values than does the transmission model. We suggest that the discrepancy of about 20% between the values calculated from the scattering model and the experimental values is due to the oversimplification in which the scattering center is infinitely small and does not affect the evanescent field distribution.

These results indicate that the scattering model is more appropriate for the photocantilever-based NSOM than is the transmission model. The photocantilever tip converts nonpropagating evanescent light into scattered light, and then the scattered light is collected by the photodiode fabricated near the cantilever tip. Since our cantilever does not have a sharp apex [Fig. 3(a)], the scattering center might be a submicron asperity. Such a small scattering center might provide the high resolution that we reported previously.[11]

III. CONCLUSION

We theoretically and experimentally investigated how nonpropagating evanescent light is converted into propagating light for a photocantilever-based NSOM. The values given by the light scattering model were closer to the experimental values than were the transmission model values. These results indicate that the photocantilever tip converts evanescent light into scattered light, which is detected by the photodiode near the cantilever tip.

ACKNOWLEDGMENTS

We would like to thank Nobuhiko Kakuta and Shinya Akamine for their aid in photocantilever fabrication. We would also like to thank Yuriko Tanaka and Hirofumi Yamada for their valuable discussions on NSOM imaging.

[1] A. Lewis, M. Isaacson, A. Hrootunian, and A. Muray, Ultramicroscopy **13**, 227 (1983).
[2] D. W. Pohl, W. Denk, and M. Lanz, Appl. Phys. Lett. **44**, 651 (1984).
[3] E. Betzig and J. K. Trautman, Science **257**, 189 (1992).
[4] F. Zenhausern, M. P. O'Boyle, and H. K. Wickramasinghe, Appl. Phys. Lett. **65**, 1623 (1994).
[5] Y. Inouye and S. Kawata, Opt. Lett. **19**, 159 (1994).
[6] R. C. Reddick, R. J. Warmack, D. W. Chilcott, S. L. Sharp, and T. L. Ferrell, Phys. Rev. B **39**, 767 (1989).
[7] S. Jiang, H. Ohsawa, K. Yamada, T. Panagaribuan, M. Ohtsu, K. Imai, and A. Ikai, Jpn. J. Appl. Phys. **31**, 2282 (1992).
[8] N. F. van Hulst, M. H. P. Moers, O. F. J. Noordman, R. G. Tack, F. B. Degerink, and B. Bolger, Appl. Phys. Lett. **62**, 461 (1993).
[9] D. Courjon, K. Sarayeddine, M. Spajer, Opt. Commun. **71**, 23 (1989).
[10] S. Akamine, H. Kuwano, K. Fukuzawa, and H. Yamada, in Proceedings of the IEEE Workshop on Micro Electro Mechanical Systems 1995, p. 145.
[11] K. Fukuzawa, Y. Tanaka, S. Akamine, H. Kuwano, and H. Yamada, J. Appl. Phys. **78**, 7376 (1995).
[12] R. C. Reddick, R. J. Warmack, D. W. Chilcot, S. L. Sharp, and T. L. Ferrell, Rev. Sci. Instrum. **61**, 3669 (1990).
[13] See, for instance, M. Born and E. Wolf, *Principles of Optics* (Pergamon, Oxford, 1975).
[14] See, for instance, J. D. Jackson, *Classical Electrodynamics* (Wiley, New York, 1962).